International Journal of Computational and Experimental Science and ENgineering (IJCESEN)

Vol. 11-No.3 (2025) pp. 4826-4834
http://www.ijcesen.com

ISSN: 2149-9144

Research Article

The Synthesis of Core-Shell Encapsulated Metal Catalysts for Conversion of Methanol to Aromatics

Hui Li*

[1]School of Chemical Engineering, Lanzhou University of Arts and Science, Lanzhou 730010, Gansu, China
***Corresponding Author Email:** i1518236380@qq.com – **ORCID:** 0000-0002-5247-7822

Article Info:

DOI: 10.22399/ijcesen.3072
Received : 21 May 2025
Accepted : 25 June 2025

Keywords

HZSM-5;
Silicalite-1;
Core-shell;
MTA;
Aromatics

Abstract:

A core-shell encapsulated metal catalyst was prepared, and its catalytic performance in the methanol-to-aromatics (MTA) reaction was investigated. This study introduces a simple secondary hydrothermal synthesis method based on the traditional preparation of HZSM-5 catalyst resulting in a nanoparticle with HZSM-5 catalyst encapsulating 2Gd%/S-1 with hollow and hierarchical pores (2Gd%/S-1@HZSM-5). This catalyst offers several advantages. First, the inner silicalite-1 layer shields the aluminum species within the HZSM-5 framework, thus passivating some of the strong acid sites on the catalyst surface. This in turn inhibits continuous reactions that result from the overly acidic surfaces. The 2Gd%/S-1@HZSM-5 catalyst demonstrates high selectivity for aromatics (59.4%), particularly BTX (benzene, toluene, and xylene), in the methanol-to-aromatics reaction (MTA). This selectivity arises from the catalyst's suitable acidity and optimized porous system. Importantly, the selectivity for C9+ aromatics is low, thus indicating effective inhibition of continuous reactions of BTX products on the catalyst surface due to low pH. Furthermore, the hydrothermal stability of the 2Gd%/S-1@HZSM-5 catalyst is significantly higher. Therefore, this method holds promise for the widespread development of novel catalysts with hollow layered porous systems, tunable pH, and high hydrothermal stability

1. Introduction

Benzene, toluene, and xylene (BTX) are raw materials used in the production of petrochemical products. These compounds are often obtained through the catalytic reforming and cracking of naphtha [1-3]. However, due to escalating oil prices worldwide, the aromatics derived from the traditional oil route often fail to meet market demands [4]. The methanol-to-aromatics (MTA) reaction has recently emerged as a promising alternative to traditional petroleum-based methods for the production of aromatics [5]. The HZSM-5 zeolite-based catalyst is widely acknowledged as the most suitable catalyst for the MTA reaction due to its unique shape-selectivity catalysis, adjustable acidity, and high hydrothermal stability [6-9]. However, traditional HZSM-5 crystals are limited by their single micropore structure and low effective diffusion length. These constraints can result in reduced catalytic efficiency due to prolonged residence times of hydrocarbon intermediates in the pores or inadequate dispersion of the product[10]. Moreover, parent HZSM-5 without loaded metal exhibits low BTX selectivity because aromatics may undergo further hydrogen transfer reactions, thus leading to the production of more alkanes [11-14]. The volatilization of metals during the reaction is also inevitable.

Core-shell structures have gained widespread attention in catalysis due to their unique properties [15]. Combining zeolite materials with the core-shell structure enables the effective utilization of zeolite's shape-selecting catalytic effect, thus allowing control over reaction selectivity and scale [16]. Tian [18-19] et al. found that treating zeolite with various organic weak bases formed hollow and hierarchical core-shell structures along with a reduction in crystal size and effective product diffusion length. The core-shell structure offers another advantage: The metal species can be fixed or encapsulated through chemical bonds or other forces to prevent the loss of active species during the reaction. Here, a 2Gd%/silicalite-1@HZSM-5 core-shell catalyst was synthesized with silicalite-1 zeolite serving as the

core. The material's catalytic performance in the MTA reaction was then characterized

2. Results and Discussion

2.1 Textural and surface properties of catalysts

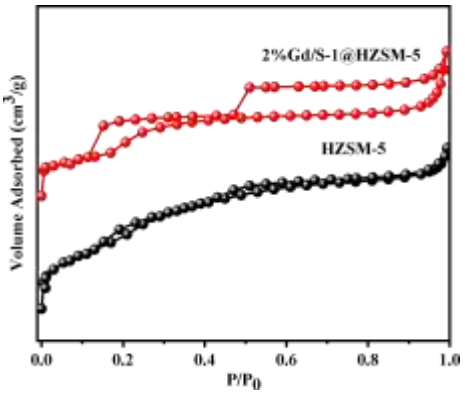

Figure 1. *N2 adsorption/desorption isotherms of all samples.*

Figure 1 illustrates the N2 adsorption/desorption isotherms of all catalysts. The specific surface area and pore volume of the modified HZSM-5 zeolite increased significantly from 175.4 m2/g to 230.5 m2/g and 0.179 cm3/g to 0.181 cm3/g, respectively, as shown in Table 2. Conversely, the specific surface area and pore volume decreased for the 2%Gd/S-1 catalyst, which could be attributed to the interface pores formed during the growth of HZSM-5 zeolite on the surface of S-1. The nitrogen adsorption increased with rising relative pressure at a P/P0 value of 0.43, thus indicating a microporous structure in the catalyst; nitrogen was adsorbed in a single layer within the micropore channel. However, at P/P0 of 0.95, the adsorption isotherm displayed a significant upturn, thus suggesting the accumulation of the catalyst samples as observed in SEM. A distinct hysteresis loop appeared in HZSM-5 at P/P0 values between 0.43 and 0.95, thus indicating capillary condensation during the desorption process and the formation of more mesoporous structures. Nitrogen could be adsorbed in multi-layer channels during this period.

SEM images of HZSM-5 and 2%Gd/S-1@HZSM-5 are shown in Figures 2(a) and (b), respectively. The synthesized HZSM-5 zeolite consists of spherical particles with uniform size but a highly rough surface. Figure1 (b) shows that the catalyst surface is smooth with noticeable growth traces after modification. Figure 1 (d) illustrates a distinct core-shell structure where a dense shell has formed on the surface of 2%Gd/S-1@HZSM-5 with obvious hollow rings. Moreover, no Gd nanoparticles were observed in TEM analysis, but the mapping diagram indicated a uniform distribution of Gd. This observation suggests the presence of an inner cladding within the core-shell structure

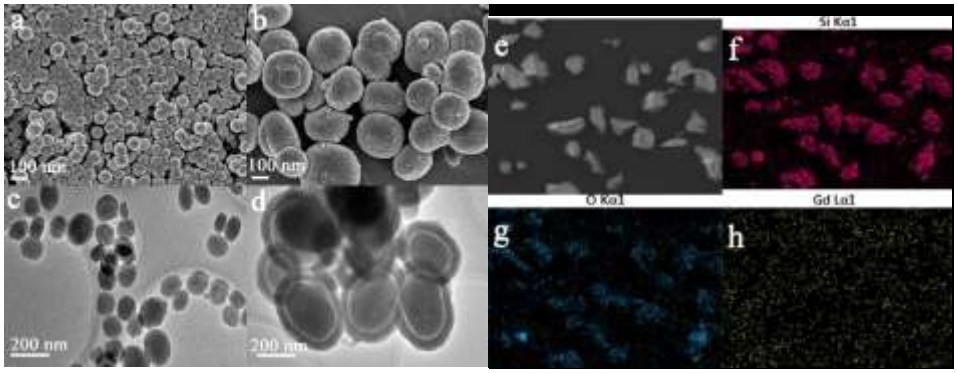

Figure 2. *(a) SEM images of HZSM-5, (b) 2%Gd/S-1@HZSM-5, (c) TEM images of HZSM-5, (d) 2%Gd/S-1@HZSM-5, and (e, f, g, h) mapping of 2%Gd/S-1@HZSM-5.*

2.2 Catalytic activity of different samples

Figure 7 shows the pyridine adsorption spectra of all catalysts. The infrared bands corresponding to the L acid site and B acid site were observed at 1453 cm−1 and 1544 cm−1, respectively. The results of pyridine adsorption for all catalysts are presented in Table 4. The quantity of L acid sites and B acid sites decreased with increasing adsorption temperature, which is consistent with the characterization results of NH3-TPD. Versus HZSM-5 zeolite, the total amount of L acid sites and B acid sites of 2%Gd/S-1@HZSM-5 catalyst decreased. This could be attributed to the S-1 zeolite being partially dissolved by the organic weak base in the mother liquor during the crystallization process. The core-shell structure of the catalyst may also play a role in XXX. Thus, the core-shell structure has impacted the quantity of L and B acid sites.

Table 1. *Distribution of products on different catalysts.*

Catalysts	Selectivity (wt. %)										Selectivity BTX (wt.%)
	C1	C2	C3	C4	C5+	B	T	X	C9+	Aromatics	
HZSM-5	2.9	11.1	9.8	18.4	16.7	12.7	9.9	15.3	3.3	41.2	37.9
2%Gd/S-1@HZSM-5	1.9	7.2	5.6	12.2	15.1	12.5	19.8	19.6	7.5	59.4	51.9

A experiment was conducted on the catalytic activity of HZSM-5 and 2%Gd/S-1@HZSM-5 in the MTA reaction. Initially, all catalysts achieved 100% conversion of methanol. The product distribution for various catalysts is presented in Table 1. The selectivity of BTX over the 2%Gd/S-1@HZSM-5 catalyst was 51.9%. Despite the low acid concentration of the 2%Gd/S-1@HZSM-5 catalyst, its unique core-shell structure generated a large number of mesopores (Figure 1). These mesopores reduced the diffusion resistance of macromolecular products facilitating the efficient conversion of reactive intermediates into aromatic products. The Py-IR results revealed a decrease in the total amount of L acid sites and B acid sites for the 2%Gd/S-1@HZSM-5 catalyst while demonstrating higher selectivity towards xylene in the MTA reaction.

Catalyst performance is likely influenced by various factors including acidity, pore structure, and morphology. A variety of hydrocarbon products can result from the conversion of methanol to aromatics. Enhancing the production of high-value aromatic products, particularly xylene, could improve the value of the MTA reaction. The activity data of the 2%Gd/S-1@HZSM-5 catalyst demonstrated that the shape-selective catalysis provided by the core-shell catalyst is particularly advantageous for generating aromatic products—especially high-value xylene.

The conversion of methanol to hydrocarbons (MTH) involves several steps including methanol to gasoline (MTG), methanol to olefin (MTO), methanol to propylene (MTP), and methanol to aromatics (MTA). Research on the MTA reaction continues due to the rapid deactivation of catalysts. It is critical to note that BTX (benzene, toluene, and xylene) serve as the intended products of MTA reactions and contribute to the creation of polycyclic aromatic hydrocarbons, which are highly active species. Therefore, it is essential to investigate methods to prevent the rapid deactivation of modified catalysts and the formation of macromolecular polycyclic aromatic hydrocarbons. Here, we examined the selectivity of BTX on various catalysts over 21 hours (Figure 3).

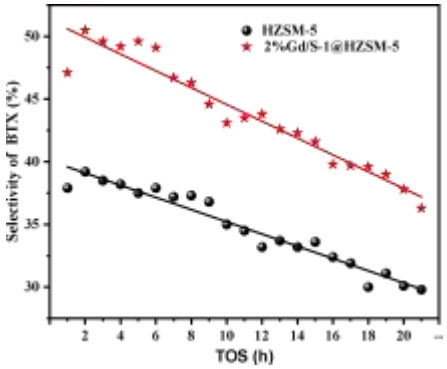

Figure 3. *Comparison of the catalytic stability of HZSM-5 and 2%Gd/S-1@HZSM-5 catalyst.*

The selectivity of BTX over HZSM-5 and 2%Gd/S-1@HZSM-5 decreases steadily with time on stream (TOS) (Figure 3). These results suggest that the acid sites on the catalyst's outer surface are effectively passivated by the core-shell structure. This allows the produced BTX to desorb quickly, thus preventing ongoing alkylation on the catalyst surface that might produce polycyclic aromatic hydrocarbons. These findings suggest that the synthesized core-shell catalyst reduces the catalyst's exterior acidity, thus reducing the rate of coke deposition.

3. Conclusion

An outer layer HZSM-5 encapsulated 2Gd%/silicalite-1 catalyst with hollow and hierarchical porous systems (2Gd%/S-1@HZSM-5) was prepared using a secondary hydrothermal synthesis method. The 2Gd%/S-1@HZSM-5 catalyst presents a three-layer structure with hierarchical porous HZSM-5 zeolite on the outside (80-100 nm thickness), a hollow structure in the middle (300-500 nm thickness), and 2Gd%/S-1 crystals inside. This structure for 2Gd%/S-1@HZSM-5 offers several advantages: The innermost silicalite-1 layer can protect the aluminum species in the framework of HZSM-5,

passivate some of the strong acid sites on the surface of HZSM-5, and inhibit the continuous reaction caused by an excessively strong acidic surface. The internal hollow system and multi-stage pore structure can minimize mass transfer resistance. The BTX selectivity of aromatic products is as high as 87.3%, while the selectivity of C9+ aromatics is extremely low. This is closely related to the reduction of the concentration of strong and weak acids in the catalyst, thus suggesting that the multifunctional catalytic system designed and synthesized can inhibit the continuous reaction of BTX products on the catalyst surface due to excessive acidity.

The 2Gd%/S-1@HZSM-5 catalyst exhibited high selectivity for aromatics (59.4%), especially BTX (51.9%), in the methanol-to-aromatics reaction (MTA) due to the suitable acidity and optimized porous system. Furthermore, the 2Gd%/S-1@HZSM-5 catalyst had much better hydrothermal stability in the MTA reaction as expected. Therefore, this method can produce novel catalysts with hollow layered porous systems, adjustable acidity, and high hydrothermal stability.

4. Experimental

4.1 Chemicals

Aluminum nitrate (AR grade) was purchased from Tianjin Shi Baishi Chemical Co., Ltd. Sodium hydroxide and ammonium nitrate were purchased from Tianjin Kemeiou Chemical Reagent Co., Ltd. Methanol (AR grade) was bought from Sinopsin Group Chemical Reagent Co., Ltd. Gadolinium nitrate hydrate (AR grade) was acquired from Alfa Aesar chemical Co., Ltd. Tetrapropylammonium hydroxide (TPAOH, 25 wt% and 40 wt% in water) and tetraethyl orthosilicate (TEOS, 99.9 wt%) were obtained from Maya Reagent.

4.2 Catalyst preparation

4.2.1 The synthesis of S-1 zeolite

A typical synthesis procedure involved adding 13.08 g of TEOS to a solution that contained 45.12 g of deionized water and 7.44 g of TPAOH. The resulting mixture was stirred for 8 h at room temperature. Subsequently, it was crystallized at 180°C for 48 h. After rapid cooling, the solid product was collected by filtration, washed with deionized water three times, and dried overnight at 110°C. The zeolite sample was obtained after calcination in air at 550°C for 4 h and labeled as S-1.

4.2.2 The synthesis of 2%Gd/S-1 samples

A 2%Gd/S-1 catalyst was prepared via the incipient wetness impregnation method. First, 0.057 g of $Gd(NO_3)_3•6H_2O$ was dissolved in 0.6 mL of deionized water; 1 g of silicalite-1 was then added to the solution. The resulting slurry was stirred at 25°C for 30 min and aged at the same temperature for 24 h. The Gd-loaded silicalite-1 sample was then prepared by calcining at 550 °C for 4 hours and drying at 110 °C for 6 hours. This catalyst was labeled as 2%Gd/S-1.

4.2.3 The synthesis of HZSM-5 zeolite

A mixture of 44.0 g of deionized water and 12.0 g of TPAOH was prepared to which 12.5 g of TEOS was added. After stirring for 8 h at room temperature, 0.46 g of $Al(NO_3)_3•9H_2O$ and 0.24 g of NaOH were added, and the mixture was stirred for an additional 30 min. The mixture was then transferred to an autoclave and crystallized at 170°C for 24 h. The resulting solids were separated and washed to neutrality. After drying at 110°C for 9 h, they were calcined at 550°C for 4 h. Finally, HZSM-5 zeolite was obtained through three ion exchange steps with 1 mol/L ammonium nitrate solution.

4.2.4 The synthesis of 2%Gd/S-1@HZSM-5

Typically, 12.5 g of TEOS was added to a mixture consisting of 11.0 g of deionized water and 12.0 g of TPAOH. After stirring for 8 h at room temperature, 0.46 g of $Al(NO_3)_3•9H_2O$ and 0.24 g of NaOH were added, and the mixture was further stirred for 30 min. Next, 0.5 g of the 2% Gd/S-1 sample was added and stirred for an additional 15 min. The resulting mixture was then transferred into an autoclave and crystallized at 170°C for 24 h. The solids were separated and washed to neutrality. After drying at 110°C for 9 h, they were calcined at 550°C for 4 h. Finally, 2% Gd/S-1@HZSM-5 was obtained via three rounds of ion exchange in 1 mol/L ammonium nitrate solution.

The hydrothermal stability of the catalysts was tested according to the literature (Figure 4)[25]. The HZSM-5 and 2%Gd/S-1@HZSM-5 catalysts were subjected to water vapor treatment in a fixed-bed reactor with a continuous flow of N_2 (20 mL/min) at 400°C for 4 h. The samples were then retrieved and labeled as HZSM-5-W and 2%Gd/S-1@HZSM-5-W, respectively

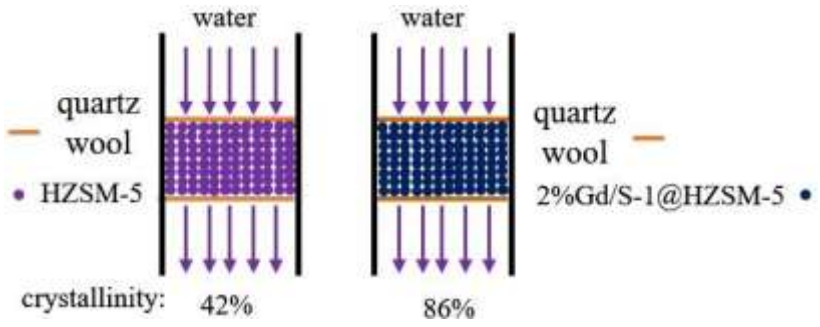

***Figure 4**. Hydrothermal stability test process.*

4.3 Catalyst characterization

A Rigaku D/Max-2400 device with a Cu Kα radiation source running at 40 kV and
150 mA was used to obtain the XRD patterns. The large-angle diffraction scanning angle (2θ) range was set between 5° and 80° with a step size of 0.02°.
The morphology of the catalysts was also characterized with a JSM-6701F scanning electron microscope (SEM) at an acceleration voltage of 15 kV. NH3 temperature-programmed desorption (NH3-TPD) measurements used an Autosorb-iQ-C chemisorption instrument from Quantachrome, USA. The Py-IR analysis was performed at two different temperatures (150°C and 350°C) on a Nicole Avatar 360 instrument. The N2 adsorption-desorption measurements were conducted at −196°C with a Micromeritics Gemini V 2380 autosorption analyzer.

4.4 Catalytic test

The performance evaluation setup for the MTA reaction catalyst is depicted in Figure 5. The MTA reaction was conducted in a fixed-bed reactor using a stainless-steel pipe (700 mm long and 10 mm wide) loaded with quartz sand. Typically, a catalyst (0.5 g) diluted with quartz sand was loaded into the stainless steel pipe, which underwent pretreatment at 400°C under a flow of N2 (20 mL/min) for 30 min. The reaction was performed at atmospheric pressure. Prior to entering the reactor, methanol was vaporized in the gasification chamber and then mixed with N2. All products were analyzed using online gas chromatographs (Tianmei GC-7890II, Shanghai) equipped with flame ionization detectors (FID). The FID was connected to SE-30 capillary columns for analysis. The carrier gas was high-purity nitrogen, and the detection conditions were as follows: column temperature 40°C, injector temperature 200°C, and detector temperature 180°C. The methanol conversion and product selectivity were calculated according to the balance of carbon atoms via formulas 1 and 2:

$$\text{Conv. methanol wt. \%} = (\text{methanol}_{\text{feed}} - \text{methanol}_{\text{off}})/\text{methanol}_{\text{feed}} \times 100\% \quad (1)$$

$$\text{Sel.i wt. \%} = A_i \times n_i / (\sum A_i \times n_i) \times 100\% \quad (2)$$

Here, A represents the peak area of the corresponding product on the gas chromatogram, and n is the number of carbon atoms of the product

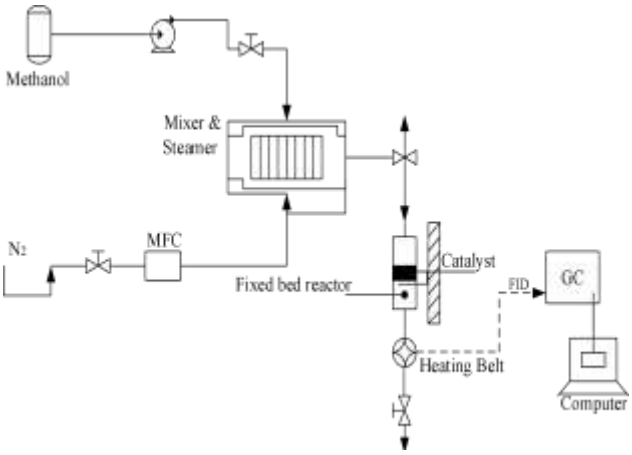

***Figure 5.** MTA reaction catalyst performance evaluation device*

Figure 6 presents the XRD patterns of all samples indicating similar diffraction peaks corresponding to the MFI structure of ZSM-5. Importantly, no characteristic Gd peak was observed in the modified sample, thus indicating a uniform dispersion of Gd species on the surface or within the pores of the zeolite. The relative crystallinities of all samples (HZSM-5, HZSM-5-W, 2%Gd/S-1@HZSM-5, and 2%Gd/S-1@HZSM-5-W) were determined to be 100%, 42%, 115%, and 86%, respectively. The higher relative crystallinity of the core-shell structure compared to the parent HZSM-5 further confirms the growth of the ZSM-5 precursor on the surface of S-1. The catalysts exhibit a considerable decrease in relative crystallinity following high-temperature water vapor treatment, which may be attributed to the

structural collapse caused by the removal of skeleton aluminum.

However, the relative crystallinity of 2%Gd/S-1@HZSM-5-W remained at 86%, which is significantly higher than HZSM-5-W indicating that the hydrothermal stability of the core-shell structure was improved versus parent HZSM-5.

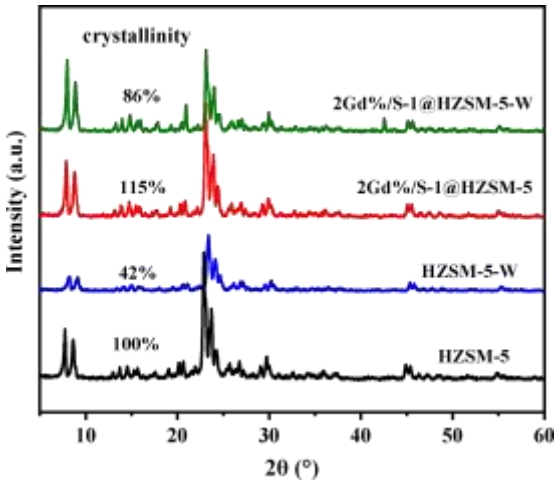

***Figure 6**. XRD patterns of all samples*

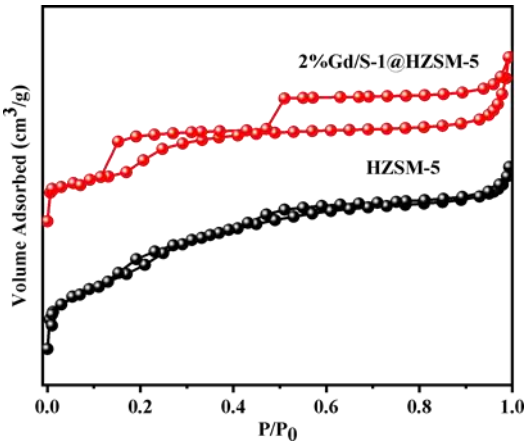

***Figure 7**. N2 adsorption/desorption isotherms of all samples.*

Figure 7 illustrates the N2 adsorption/desorption isotherms of all catalysts. The specific surface area and pore volume of the modified HZSM-5 zeolite increased significantly from 175.4 m2/g to 230.5 m2/g and 0.179 cm3/g to 0.181 cm3/g, respectively (Table 2). Conversely, the specific surface area and pore volume decreased for the 2%Gd/S-1 catalyst, which could be attributed to the interface pores formed during the growth of HZSM-5 zeolite on the surface of S-1.

Nitrogen adsorption increased with the rise in relative pressure over the P/P0 range of 0.43, which indicated a microporous structure in the catalyst with nitrogen being adsorbed in a single layer within the micropore channels. At P/P0 about 0.95, however, the adsorption isotherm showed a significant upturn, thus suggesting the accumulation of the catalyst samples as also seen in SEM. Furthermore, for P/P0 values between 0.43 and 0.95, a distinct hysteresis loop appeared in HZSM-5, thus indicating capillary condensation during the desorption process and the formation of more mesoporous structures. Nitrogen could be adsorbed in multi-layer channels during this period.

Figure 8 illustrates the acidity and concentration distribution of HZSM-5 and 2%Gd/S-1@HZSM-5. The NH3-TPD curves of all samples show two desorption peaks representing the weak and strong acid positions of the catalyst. Table 3 shows that the core-shell structure had a profound impact on the weak and strong acid strengths of the catalyst. Versus the parent HZSM-5 zeolite, the peak areas corresponding to the weak and strong acid desorption peaks were significantly reduced in the core-shell structure, thus suggesting a decrease in the acid concentration of the catalyst. This reduction could be attributed to the coverage of the acidic sites in the shell HZSM-5 by the core layer.

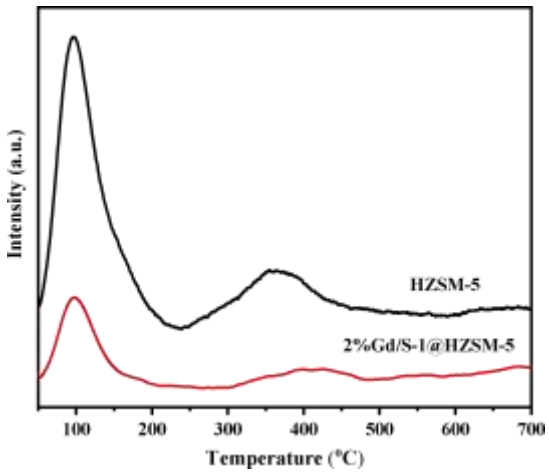

***Figure 8**. NH3-TPD profiles of all samples.*

Figure 9 displays the pyridine adsorption spectra of all catalysts. The infrared bands corresponding to the L acid site and B acid site were observed at 1453 cm−1 and 1544 cm−1, respectively. The results of pyridine adsorption for all catalysts are presented in Table 4. The quantity of L acid sites and B acid sites decreased with increasing adsorption temperature, which is consistent with the characterization results of NH3-TPD. Versus HZSM-5 zeolite, the number of L acid sites and B acid sites decreased in 2%Gd/S-1@HZSM-5 catalyst. This could be attributed to the S-1 zeolite being partially dissolved by the organic weak base in the mother liquor during crystallization. The core-shell structure of the catalyst may also play a crucial role. Thus, the core-shell structure has a considerable impact on the quantity of L and B acid sites.

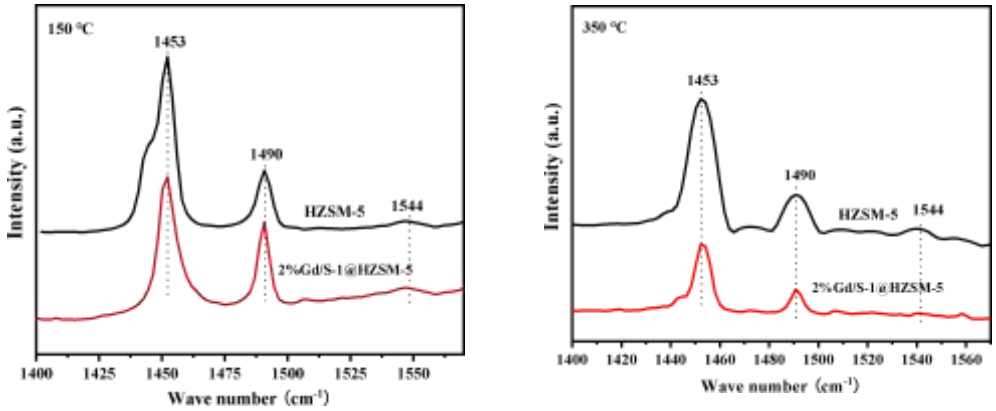

***Figure 9**. IR spectra of pyridine adsorption for all samples*

***Table 2**. Porosity analysis*

Samples	S_{BET} [a]	S_{micro} [b]	S_{meso} [c]	V_{total} [d]	V_{micro} [e]	V_{meso} [f]
	(m^2/g)	(m^2/g)	(m^2/g)	(cm^3/g)	(cm^3/g)	(cm^3/g)
HZSM-5	398.3	222.9	175.4	0.267	0.088	0.179
2%Gd/S-1@HZSM-5	387.1	156.6	230.5	0.251	0.070	0.181

Note: [a] BET method; [b] t-plot method; [c] S_{meso} = SBET-Smicro; [d] volume adsorbed at P/P_0 = 0.99; [e] t-plot method; [f] V_{meso} = V_{total}-V_{micro}

***Table 3**. Summary catalyst acidity*

samples	Acid sites (mmol/g)		
	Weak	Strong	Total
HZSM-5	0.317	0.187	0.504
2%Gd/S-1@HZSM-5	0.112	0.017	0.129

***Table 4**. Summary catalyst acidity.*

samples	Weak acid sites[a] (a.u/g)			Strong acid sites[a] (a.u/g)		
	Lewis	Brønsted	total	Lewis	Brønsted	total
HZSM-5	234.4	17.9	252.3	31.9	4.7	36.6
2%Gd/S-1@HZSM-5	227.8	13.0	240.8	14.3	7.1	21.4

[a]The quantity of the weak and strong acid sites were determined by Py-IR; the strong acid sites were obtained from Py-IR spectra at 350°C, and the weak acid sites were calculated by subtracting the acid quantity at 350°C from the acid quantity at 150°C.

Author Statements

- **Ethical approval:** The conducted research is not related to either human or animal use.
- **Conflict of interest:** The authors declare that they have no known competing financial interests or personal relationships that could have appeared to influence the work reported in this paper
- **Acknowledgement:** The authors declare that they have nobody or no-company to acknowledge.
- **Author contributions:** The authors declare that they have equal right on this paper.
- **Funding information:** The authors declare that there is no funding to be acknowledged.
- **Data availability statement:** The data that support the findings of this study are available on request from the corresponding author. The data are not publicly available due to privacy or ethical restrictions

References

[1] Ji, Y. J., Zhang, B., Xu, L., Wu, H. H., Peng, H. G., Chen, L. Y., Liu, M., Wu, P., (2011). Core/shell-structured Al-MWW@B-MWW zeolites for shape-selective toluene disproportionation to para-xylene. *J. Catal*. 283; 168-177.

[2] Zhao, Y., Wu, H., Tan, W., Zhang, M., Guo, X., (2010). Effect of metal modification of HZSM-5 on catalyst stability in the shape-selective methylation of toluene. *Catal. Today*, 156; 69-73.

[3] Li, J., Xiang, H., Liu, M., Wang, Q., Zhu, Z., Hu, Z., (2014). The deactivation mechanism of two typical shape-selective HZSM-5 catalysts for alkylation of toluene with methanol. *Catal. Sci. Technol*. ;4 2639-2649.

[4] Song, Y., Sun, C., Shen, W., Lin, L., (2007). Hydrothermal post-synthesis of HZSM-5 zeolite to enhance the coke-resistance of Mo/HZSM-5 catalyst for methane dehydroaromatization reaction: reconstruction of pore structure and modification of acidity. *Appl. Catal*. A, 317; 266-274.

[5] Sun, X., Mueller, S., Liu, Y., Shi, H., Haller, G. L., Sanchez-Sanchez, M., (2014). On reaction pathways in the conversion of methanol to hydrocarbons on HZSM-5. *J. Catal*. 317; 185-197.

[6] Lopez-Sanchez, J. A., Conte, M., Landon, P., Zhou, W., Bartley, J. K., Taylor, S. H., (2012). Reactivity of Ga2O3 clusters on zeolite ZSM-5 for the conversion of methanol to aromatics. *Catal. Lett*. 142; 1049-1056.

[7] Chen, Z. Y, Ni, Y. M., Zhi, Y. C., Wen, F. L., Zhou, Z. Q., Wei, Y. G., Zhu, W. L., Liu, Z. M., (2018). Coupling of methanol and carbon monoxide over HZSM-5 to form aromatics. Angew. *Chem. Int. Edit*. 57; 12549-12553.

[8] Niu, X., Gao, J., Miao, Q., Dong, M., Wang, G., Fan, W., (2014). Influence of preparation method on the performance of Zn-containing HZSM-5 catalysts in methanol-to-aromatics. *Micropor. Mesopor. Mat.* 197; 252-261.

[9] Liang, T., Chen, J., Qin, Z., Li, J., Wang, P., Wang, S., (2016). Conversion of methanol to olefins over HZSM-5 zeolite: reaction pathway is related to the framework aluminum siting. *ACS Catal*. 6; 7311-7325.

[10] Zhang, J., Qian, W., Kong, C., Wei, F., (2015). Increasing para-xylene selectivity in making aromatics from methanol with a surface-modified Zn/P/ZSM-5 catalyst. *ACS Catal*, 5; 2982-2988.

[11] Lee, S., Choi, M.,)2019). Unveiling coke formation mechanism in MFI zeolites during methanol-to-hydrocarbons conversion. *J. Catal*. 375; 183-192.

[12] Wang, N., Hou, Y., Sun, W., Cai, D., Chen, Z., Liu, L., (2019). M. (2013). Catalyst deactivation by coke formation in microporous and desilicated zeolite HZSM-5 during the conversion of methanol to hydrocarbons. J. *Catal*. 307; 62-73.

[14] Wang, K., Dong, M., Niu, X., Li, J., Qin, Z., Fan, W., (2018). Highly active and stable Zn/ZSM-5 zeolite catalyst for the conversion of methanol to aromatics: effect of support morphology. *Catal. Sci. Technol*. 8; 5646-5656.

[15] Wan, W., Fu, T., Qi, R., Shao, J., Li, Z., (2016). Co-effect of Na+ and TPA+ in alkali treatment on fabrication of mesoporous ZSM-5 catalyst for methanol to hydrocarbons reaction. *Ind. Eng. Chem. Res.* 55; 13040-13049.

[16] Conte, M., Lopez-Sanchez, J. A., He, Q., Morgan, D. J., (2011). Hutchings, G. J., Modified zeolite ZSM-5 for the methanol to aromatics reaction. *Catal. Sci. Technol.* 2; 105-112.

[17] Ni, Y., Zhu, W., Liu, Z., (2021). Formaldehyde intermediate participating in the conversion of methanol to aromatics over zinc modified HZSM-5. *J. Energy Chem*. 54; 174-178.

[18] Dong, P., Zhang, Y., Li, Z., Yong, H., Li, G., Ji, D., (2019). Enhancement of the utilization of methanol in the alkylation of benzene with methanol over 3-aminopropyltriethoxysilane modified HZSM-5. *Catal. Commun*. 123; 6-10.

[19] Tian, H., Lv, J., Liang, X., Tang, X., Zha, F., (2018). Tuning morphology of Zn/HZSM-5 on catalytic performance in methanol aromatization. Energy Technol-Ger., 6; 1986-1993.

[20] Li, G. X., Wu, C., Dong, P., Ji, D., Zhang, Y. F, (2020). Core-shell HZSM-5@silicalite-1 composite: controllable synthesis and catalytic performance in alkylation of toluene with methanol. *Catal. Lett*. 150; 1923-1931.

[21] Wang, X. Y., Wen, M., Wang, C. Z., Ding, J., Sun, Y., Liu, Y., (2014). Microstructured fiber@HZSM-5 core-shell catalysts with dramatic selectivity and stability improvement for the methanol-to-propylene process. *Chem. Commun*. 50; 6343-6345.

[22] Jin, Z., Liu, S., Qin, L., Liu, Z., Wang, Y., Xie, Z., (2013). Methane dehydroaromatization by Mo-supported MFI-type zeolite with core-shell structure. *Appl. Catal. A-Gen*. 453; 295-301.

[23] Kong, D., Liu, Z., Fang, D., (2009). Epitaxial growth of core-shell ZSM-5/silicalite-1 with shape selectivity. *Chinese J. Catal*. 30; 885-890.

[24] Khaledi, K., Haghighi, M., Sadeghpour, P., (2017(. On the catalytic properties and performance of core-shell ZSM-5@MnO nanocatalyst used in conversion of methanol to light olefins. *Micropor. Mesopor. Mat.*, 246, 51-61.

[25] Wu, Y., Li, J., Chai, Y., Guo, H., Liu, C., (2015). Synergetic effect of HZSM-5/silicalite-1@Pt/Al2O3 core-shell catalyst to enhance the selective hydrogenation of p-xylene. *J. Membrane Sci.* 496; 70-77.